Appendix

Table of Contents

A Notations **15**

B Review of the cold-start issue in link prediction and recommender systems **16**

C Link-centric and Node-centric Evaluation Metrics **17**
C.1 Link-Centric Evaluation 17
C.2 Node-Centric Evaluation 17

D Proof of Theorems **18**
D.1 Approximation power of ATC for TC 18
D.2 Degree-related Bias of Evaluation Metrics 19
D.3 Reweighting by LP Score Enhance 1-layer TC 21

E Example demonstrating the advantages of TC over LCC **22**

F Datasets and Experimental Settings **23**
F.1 Dataset Introduction and Statistics 23
F.2 Hyperparameter Details 23

G Additional Results **24**
G.1 Link prediction performance grouped by TC^{Test} 24
G.2 Link prediction performance grouped by TC^{Train} 25
G.3 Link prediction performance grouped by $Degree^{Test}$ 26
G.4 Link prediction performance grouped by $Degree^{Train}$ 27
G.5 Relation between LP performance and TC at Graph-level 28
G.6 Relation between TC^{Train} and TC^{Test} 28
G.7 Difference in TC vs Difference in Performance before/after applying reweighting 28
G.8 Correlation of the performance with TC and Degree 28

H Edge Reweighting Algorithm **37**

I Reweigh edges for baselines without message-passing **37**

J Comparing the Efficiency between baseline and their augmented version by TC **38**

K Reweighting training neighbors based on their connections to training neighbors or validation neighbors **38**

L Explaining why the curve of link prediction performance has several fast down in Figure 7 (a) **39**

A NOTATIONS

This section summarizes notations used throughout this paper.

Table 2: Notations used throughout this paper.

Notations	Definitions or Descriptions
$G = (\mathcal{V}, \mathcal{E}, \mathbf{X})$	Graph with node set $\mathcal{V}$, edge set $\mathcal{E}$ and node feature $\mathbf{X}$
m, n	Number of nodes $m = \lvert\mathcal{V}\rvert$ and number of edges $n = \lvert\mathcal{E}\rvert$
v_i, e_{ij}	Node v_i and the edge e_{ij} between node v_i and v_j
$\mathbf{A}$	Adjacency matrix $\mathbf{A}_{ij} = 1$ indicates an edge e_{ij} between v_i, v_j
$\widetilde{\mathbf{A}}$	Row-based normalized graph adjacency matrix $\widetilde{\mathbf{A}} = \mathbf{D}^{-1}\mathbf{A}$
$\widehat{\mathbf{A}}$	GCN-based normalized graph adjacency matrix $\widehat{\mathbf{A}} = \mathbf{D}^{-0.5}\mathbf{A}\mathbf{D}^{-0.5}$
$\widetilde{\mathbf{A}}^t$	Updated adjacency matrix at iteration t
$\mathbf{D}$	Diagonal degree matrix $\mathbf{D}_{ii} = \sum_{j=1}^{n} \mathbf{A}_{ij}$
$\widehat{d}$	Average degree of the network
$\mathcal{T} = \{\text{Train}, \text{Val}, \text{Test}\}$	Set of Training/Validation/Testing edge groups
$\text{Degree}^{\text{Train/Val/Test}}$	Degree based on Training/Validation/Testing Edges
$\text{TC}^{\text{Train/Val/Test}}$	Topological Concentrations that quantify intersections with Training/Validation/Testing neighbors
$\mathcal{N}_i^t$	Node v_i's 1-hop neighbors of type $t, t \in \mathcal{T}$
$\mathcal{H}_i^k$	Nodes having at least one path of length k to v_i based on training edges $\mathcal{E}^{\text{Train}}$
$\mathcal{S}_i^K = \{\mathcal{H}_i^k\}_{k=1}^K$	K-hop computational tree centered on the node v_i
$C_i^{K,t} \backslash \widetilde{C}_i^{K,t}$	(Approximated) Topological concentration for node v_i considering the intersection among K-hop computational trees among its type t neighbors.
$\mathbf{E}_i^k$	Embedding of the node v_i after k^{th}-layer message-passing
$\mathbf{R}_{ij}$	Sample from gaussian random variable $\mathcal{N}(0, 1/d)$
$g_{\mathbf{\Theta}_g}$	Link predictor parameterized by $\mathbf{\Theta}_g$
$\widetilde{\mathcal{E}}_i, \widehat{\mathcal{E}}_i$	Predicted and ground-truth neighbors of node v_i
$\mathcal{HG}$	Hypergeometric distribution
LP	Link Prediction
(A)TC	(Approxminated) Topological Concentration
TDS	Topological Distribution Shift
β	Exponential discounting effect as the hop increases
α_k	Weighted coefficient of layer k in computing ATC
μ	Mean of the distribution
L	Number of message-passing layers
γ	Coefficients measuring the contribution of updating adjacency matrix

B REVIEW OF THE COLD-START ISSUE IN LINK PREDICTION AND RECOMMENDER SYSTEMS

One line of the research (Leroy et al., 2010; Ge & Zhang, 2012; Yan et al., 2013; Han et al., 2015; Wang et al., 2016; Xu et al., 2017) defines the cold-start nodes as the ones with little to no topological information (isolated user) and augment these disadvantaged groups with auxiliary information, e.g., user profile/rich text information, community information, and group membership. Specifically, (Yan et al., 2013) derive the auxiliary information based on the interactions of these disadvantageous nodes/users from their cross-platform behaviors. (Leroy et al., 2010) constructs the probabilistic graph and then refines it by considering the transitivity of the contract relationship. (Ge & Zhang, 2012) incorporates feature selection and regularization to avoid overfitting. The other line of research (Wang et al., 2019; Dong et al., 2020; Li et al., 2021; Hao et al., 2021; Rahmani et al., 2022; Wei & He, 2022) studies the cold-start issue from the user perspective in recommender systems. They usually define cold-start nodes/users as the ones with no-to-sparse/low activities. (Li et al., 2021; Rahmani et al., 2022) devises a re-ranking strategy by optimizing the performance gap between low-activity and high-activity users. (Dong et al., 2020; Wei & He, 2022) design multiple meta-learning frameworks to learn user preferences based on his/her few past interactions. (Wang et al., 2019) uses knowledge graph embedding to assist with recommendation tasks for low-activity users while (Hao et al., 2021) trains GNNs to adapt to cold-start nodes by mimicking the cold-start scenario for warm users.

Following the above second line of research, we study the cold-start link prediction at the node level since our paper targets demystifying the varying link prediction performance across different nodes. Therefore, we follow some conventional literature (Wang et al., 2019; Dong et al., 2020; Li et al., 2021; Wei & He, 2022) and deem the nodes with generally few degrees as cold-start ones. Particularly, in Figure 4(b)/(e), we change the degree threshold from 1 to 10, divide nodes into two groups at each degree threshold, and further visualize the average performance for each group. We can see that nodes in the lower-degree groups generally have higher performance than nodes in the higher-degree groups. The above observation has two promising insights compared with conventional literature:

- **(1)** Many existing recommendation-based papers (Wang et al., 2019; Dong et al., 2020; Li et al., 2021; Newman, 2001) define cold-start users/nodes as the ones with few/little interactions/topological signals. However, our paper empirically demonstrates that nodes with lower degrees even exhibit higher LP performance.
- **(2)** Many existing node classification papers (Tang et al., 2020; Chen et al., 2021a; Wang et al., 2022a) find nodes with low degrees have lower performance. However, our work sheds new insights into the degree-related bias in link prediction where nodes with lower degrees can actually possess higher performance.

We justify the above 1st insight by relating to real-world scenarios where users with high degrees usually tend to possess diverse interests (nodes with higher degrees may tend to belong to diverse communities) and therefore, using the equal capacity of embedding cannot equally characterize all of their interests (Zhao et al., 2021d).

We justify the above 2nd insight by relating to the inherent difference between the mechanism of node classification and the mechanism of link prediction. For node classification, high-degree nodes are more likely to obtain the supervised signals from labeled nodes in the same class (Chen et al., 2021a). For link prediction, the ground-truth class for each node is actually its testing neighbors and hence when performing message-passing, beneficial supervision signals are not guaranteed to be captured more by high-degree nodes.

In our paper, we focus on the performance difference between low-degree nodes and high-degree nodes rather than the cold-start issue. However, if we also consider cold-start nodes as the ones with sparse interactions as some previous work did (Li et al., 2021; Rahmani et al., 2022), then our analysis and observation can also apply there.

C LINK-CENTRIC AND NODE-CENTRIC EVALUATION METRICS

In addition to the conventional link-centric evaluation metrics used in this work, node-centric evaluation metrics are also used to mitigate the positional bias caused by the tiny portion of the sampled negative links. We introduce their mathematical definition respectively as follows:

C.1 LINK-CENTRIC EVALUATION

Following (Hu et al., 2020), we rank the prediction score of each link among a set of randomly sampled negative node pairs and calculate the link-centric evaluation metric Hits@K as the ratio of positive edges that are ranked at K^{th}-place or above. Note that this evaluation may cause bias as the sampled negative links only count a tiny portion of the quadratic node pairs (Li et al., 2023). Hereafter, we introduce the node-centric evaluation metrics and specifically denote the node-level Hit ratio as Hits^N@K to differentiate it from the link-centric evaluation metric Hits@K.

C.2 NODE-CENTRIC EVALUATION

For each node $v_i \in \mathcal{V}$, the model predicts the link formation score between v_i and *every other node*, and selects the top-K nodes to form the potential candidates $\widetilde{\mathcal{E}}_i$. Since the ground-truth candidates for node v_i is $\mathcal{N}_i^{\text{Test}}$ (hereafter, we notate as $\widehat{\mathcal{E}}_i$), we can compute the Recall (R), Precision (P), F1, NDCG (N), MRR and Hits^N of v_i as follows:

$$\text{R@}K_i = \frac{|\widetilde{\mathcal{E}}_i \cap \widehat{\mathcal{E}}_i|}{|\widehat{\mathcal{E}}_i|}, \qquad \text{P@}K_i = \frac{|\widetilde{\mathcal{E}}_i \cap \widehat{\mathcal{E}}_i|}{K} \tag{5}$$

$$\text{F1@}K_i = \frac{2|\widetilde{\mathcal{E}}_i \cap \widehat{\mathcal{E}}_i|}{K + |\widehat{\mathcal{E}}_i|}, \qquad \text{N@}K_i = \frac{\sum_{k=1}^{K} \frac{\mathbb{1}[v_{\phi_i^k} \in (\widetilde{\mathcal{E}}_i \cap \widehat{\mathcal{E}}_i)]}{\log_2(k+1)}}{\sum_{k=1}^{K} \frac{1}{\log_2(k+1)}} \tag{6}$$

$$\text{MRR@}K_i = \frac{1}{\min_{v \in (\widetilde{\mathcal{E}}_i \cap \widehat{\mathcal{E}}_i)} \text{Rank}_v}, \qquad \text{Hits}^N\text{@}K_i = \mathbb{1}[|\widehat{\mathcal{E}}_i \cap \widetilde{\mathcal{E}}_i| > 0], \tag{7}$$

where ϕ_i^k denotes v_i's k^{th} preferred node according to the ranking of the link prediction score, Rank_v is the ranking of the node v and $\mathbb{1}$ is the indicator function equating 0 if the intersection between $\widehat{\mathcal{E}}^i \cap \widetilde{\mathcal{E}}_i$ is empty otherwise 1. The final performance of each dataset is averaged across each node:

$$\text{X@}K = \mathbb{E}_{v_i \in \mathcal{V}} X\text{@}K_i, \text{X} \in \{\text{R}, \text{P}, \text{F1}, \text{N}, \text{MRR}, \text{Hits}^N\} \tag{8}$$

Because for each node, the predicted neighbors will be compared against all the other nodes, there is no evaluation bias compared with the link-centric evaluation where only a set of randomly selected negative node pairs are used.

D PROOF OF THEOREMS

D.1 APPROXIMATION POWER OF ATC FOR TC

Theorem 1. *Assuming $g(|\mathcal{H}_i^{k_1}|, |\mathcal{H}_j^{k_2}|) = |\mathcal{H}_i^{k_1}||\mathcal{H}_j^{k_2}|$ in Eq. (1) and let ϕ be the dot-product based similarity metric (He et al., 2020), then node v_i's 1-layer Topological Concentration $C_i^{1,t}$ is linear correlated with the mean value of the 1-layer Approximated Topological Concentration $\mu_{\widetilde{C}_i^{K,t}}$ as:*

$$C_i^{1,t} \approx d^{-1}\mu_{\mathbb{E}_{v_j\sim\mathcal{N}_i^t}(\mathbf{E}_j^1)^\top\mathbf{E}_i^1} = d^{-1}\mu_{\widetilde{C}_i^{1,t}}, \tag{9}$$

where $\mathbf{E}^1 \in \mathbb{R}^{n\times d}$ denotes the node embeddings after 1-layer SAGE-style message-passing over the node embeddings $\mathbf{R} \sim \mathcal{N}(\mathbf{0}^d, \mathbf{\Sigma}^d)$.

Proof. Assuming without loss of generalizability that the row-normalized adjacency matrix $\widetilde{\mathbf{A}} = \mathbf{D}^{-1}\mathbf{A}$ is used in aggregating neighborhood embeddings. We focus on a randomly selected node $\mathbf{E}_i \in \mathbb{R}^d, \forall v_i \in \mathcal{V}$ and its 1-layer ATC given by Eq. (2) is:

$$\begin{aligned}
\widetilde{C}_i^{1,t} = \mathbb{E}_{v_j\sim\mathcal{N}_i^t}(\mathbf{E}_j^1)^\top\mathbf{E}_i^1 &= \mathbb{E}_{v_j\sim\mathcal{N}_i^t}(\widetilde{\mathbf{A}}\mathbf{R})_j^\top(\widetilde{\mathbf{A}}\mathbf{R})_i \\
&= \mathbb{E}_{v_j\sim\mathcal{N}_i^t}\frac{1}{|\mathcal{N}_j^{\text{Train}}||\mathcal{N}_i^{\text{Train}}|}\Big(\sum_{v_m\in\mathcal{N}_j^{\text{Train}}}\mathbf{R}_m\Big)^\top\Big(\sum_{v_n\in\mathcal{N}_i^{\text{Train}}}\mathbf{R}_n\Big) \\
&= \mathbb{E}_{v_j\sim\mathcal{N}_i^t}\frac{1}{|\mathcal{N}_j^{\text{Train}}||\mathcal{N}_i^{\text{Train}}|}\sum_{(v_m,v_n)\in\mathcal{N}_j^{\text{Train}}\times\mathcal{N}_i^{\text{Train}}}(\mathbf{R}_m)^\top\mathbf{R}_n \\
&= \mathbb{E}_{v_j\sim\mathcal{N}_i^t}\frac{1}{|\mathcal{H}_i^1||\mathcal{H}_j^1|}\Big(\underbrace{\sum_{\substack{(v_m,v_n)\in\mathcal{N}_j^{\text{Train}}\times\mathcal{N}_i^{\text{Train}},\\ v_m\neq v_n}}(\mathbf{R}_m)^\top\mathbf{R}_n}_{\text{Non-common neighbor embedding pairs}} + \underbrace{\sum_{v_k\in\mathcal{N}_j^{\text{Train}}\cap\mathcal{N}_i^{\text{Train}}}(\mathbf{R}_k)^\top\mathbf{R}_k}_{\text{Common neighbor embedding pairs}}\Big),
\end{aligned} \tag{10}$$

Note that the first term is the dot product between any pair of two non-common neighbor embeddings, which is essentially the dot product between two independent samples from the same multivariate Gaussian distribution (*note that here we do not perform any training optimization, so the embeddings of different nodes are completely independent*). By central limit theorem (Kwak & Kim, 2017), the first term approaches the standard Gaussian distribution with 0 as the mean, *i.e.*, $\mu_{(\mathbf{R}_m)^\top\mathbf{R}_n} = 0$. In contrast, the second term is the dot product between any Gaussian-distributed sample and itself, which can be essentially characterized as the sum of squares of d independent standard normal random variables and hence follows the chi-squared distribution with d degrees of freedom, i.e., $(\mathbf{R}_k)^\top\mathbf{R}_k \sim \chi_d^2$ (Sanders, 2009). By Central Limit Theorem, $\lim_{d\to\infty} P(\frac{\chi_d^2-d}{\sqrt{2d}} \leq z) = P_{\mathcal{N}(0,1)}(z)$ and hence $\lim_{d\to\infty}\chi_d^2 = \mathcal{N}(d, 2d), i.e., \mu_{(\mathbf{R}_k)^\top\mathbf{R}_k} = d$. Then we obtain the mean value of $\mathbb{E}_{v_j\sim\mathcal{N}_i^t}(\mathbf{E}_j^1)^\top\mathbf{E}_i^1$:

$$\begin{aligned}
\mu_{\widetilde{C}_i^{1,t}} = \mu_{\mathbb{E}_{v_j\sim\mathcal{N}_i^t}(\mathbf{E}_j^1)^\top\mathbf{E}_i^1} &\approx \mathbb{E}_{v_j\sim\mathcal{N}_i^t}\frac{1}{|\mathcal{H}_i^1||\mathcal{H}_j^1|}\Big(\mu_{\sum_{\substack{(v_m,v_n)\in\mathcal{N}_j^{\text{Train}}\times\mathcal{N}_i^{\text{Train}},\\ v_m\neq v_n}}(\mathbf{R}_m)^\top\mathbf{R}_n} + \mu_{\sum_{v_k\in\mathcal{N}_j^{\text{Train}}\cap\mathcal{N}_i^{\text{Train}}}(\mathbf{R}_k)^\top\mathbf{R}_k}\Big) \\
&\approx \mathbb{E}_{v_j\in\mathcal{N}_i^t}\frac{d|\mathcal{N}_i^{\text{Train}}\cap\mathcal{N}_j^{\text{Train}}|}{|\mathcal{H}_i^1||\mathcal{H}_j^1|} = \mathbb{E}_{v_j\in\mathcal{N}_i^t}\frac{d|\mathcal{H}_i^1\cap\mathcal{H}_j^1|}{|\mathcal{H}_i^1||\mathcal{H}_j^1|} = dC_i^{1,t}.
\end{aligned} \tag{11}$$

The first approximation holds if assuming all nodes share the same degree. The second approximation holds since we set d to be at least 64 for all experiments in this paper. We next perform Monte-Carlo Simulation to verify that by setting $d = 64$, the obtained distribution is very similar to the Gaussian distribution. Assuming without loss of generality that the embedding dimension is 64 with the mean vector $\boldsymbol{\mu} = \mathbf{0}^{64} \in \mathbb{R}^{64}$ and the identity covariance matrix $\mathbf{\Sigma}^{64} = \mathbf{I} \in \mathbb{R}^{64\times64}$, we randomly sample 1000 embeddings from $\mathcal{N}(\boldsymbol{\mu}, \mathbf{\Sigma})$.

We visualize the distributions of the inner product between the pair of non-common neighbor embeddings, i.e., the first term in Eq. (10) $(\mathbf{R}_m)^\top \mathbf{R}_n, v_m \neq v_n$, and the pair of common neighbor embeddings, i.e., the second term in Eq. (10) $(\mathbf{R}_k)^\top \mathbf{R}_k, v_k \in \mathcal{N}_j^{\text{Train}} \cap \mathcal{N}_i^{\text{Train}}$ in Figure 8. We can see that the distribution of the dot product between the pair of non-common neighbor embeddings behaves like a Gaussian distribution centering around 0. In contrast, the distribution of the dot product between the pair of common neighbor embeddings behaves like a chi-square distribution of degree 64, which also centers around 64, and this in turn verifies the Gaussian approximation. Note that the correctness of the first approximation in Eq. (11) relies on the assumption that the average of the inverse of the node's neighbors should be the same across all nodes. Although it cannot be theoretically satisfied, we still empirically verify the positive correlation between TC and the link prediction performance shown in Figure 3.

The above derivation bridges the gap between the Topological Concentration (TC) defined in the topological space and the Approximated Topological Concentration (ATC) defined in the latent space, which theoretically justifies the approximation efficacy of ATC. □

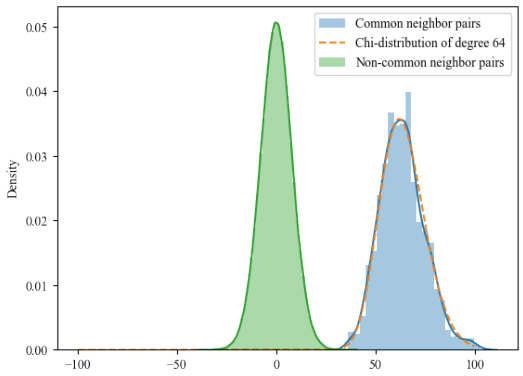

Figure 8: The distribution of the inner product between common neighbor pairs is statistically higher than that between non-common neighbor pairs.

D.2 Degree-related Bias of Evaluation Metrics

One previous work (Wang & Derr, 2022) has empirically shown the degree-related bias of evaluation metrics used in link prediction models. Following that, we go one step further and theoretically derive the concrete format of the evaluation bias in this section. We leverage an untrained link prediction model to study the bias. This avoids any potential supervision signal from training over observed links and enables us to study the evaluation bias exclusively. Since two nodes with the same degree may end up with different performances, i.e., $\text{X@}K_i \neq \text{X@}K_j, d_i = d_j$, we model $\text{X@}K|d$ as a random variable and expect to find the relationship between its expectation and the node degree d, i.e., $f : E(\text{X@}K|d) = f(d)$.

Following many existing ranking works (He et al., 2020; Chen et al., 2021b), we assume without loss of generalizability that the link predictor $\mathscr{P}$ ranking the predicted neighbors based on their embedding similarity with embeddings noted as $\mathbf{E}$, then we have:

Lemma 1. *For any untrained embedding-based link predictor $\mathscr{P}$, given the existing $k-1$ predicted neighbors for the node $v_i \in \mathcal{V}$, the k^{th} predicted neighbor is generated by randomly selecting a node without replacement from the remaining nodes with equal opportunities, i.e.,* $P(v_{\phi_i^k} = v | \{v_{\phi_i^1}, v_{\phi_i^2}, ..., v_{\phi_i^{k-1}}\}) = \frac{1}{N-(k-1)}$.

Without any training, Lemma 1 trivially holds since embeddings of all nodes are the same, which trivially leads to the following theorem:

Theorem 2. *Given the untrained embedding-based link predictor $\mathscr{P}$, the size of the intersection between any node's predicted list $\widetilde{\mathcal{E}}_i$ and its ground-truth list $\widehat{\mathcal{E}}_i$ follows a hypergeometric distribution: $|\widetilde{\mathcal{E}}_i \cap \widehat{\mathcal{E}}_i| \sim \mathcal{HG}(|\mathcal{V}|, K, |\widehat{\mathcal{E}}_i|)$ where $|\mathcal{V}|$ is the population size (the whole node space), K is*

the number of trials and $|\widehat{\mathcal{E}}_i|$ is the number of successful states (the number of node's ground-truth neighbors).

Proof. Given the ground-truth node neighbors $\widehat{\mathcal{E}}_i$, the predicted neighbors $\widetilde{\mathcal{E}}_i = \{v_{\phi_i^k}\}_{k=1}^K$ is formed by selecting one node at a time without replacement K times from the whole node space $\mathcal{V}$. Since any selected node $v_{\phi_i^k}$ can be classified into one of two mutually exclusive categories $\widehat{\mathcal{E}}_i$ or $\mathcal{V}\backslash\widehat{\mathcal{E}}_i$ and by Lemma 1, we know that for any untrained link predictor, each unselected node has an equal opportunity to be selected in every new trial, we conclude that $|\widetilde{\mathcal{E}}_i \cap \widehat{\mathcal{E}}_i| \sim \mathcal{HG}(|\mathcal{V}|, K, |\widehat{\mathcal{E}}_i|)$ and by default $E(|\widetilde{\mathcal{E}}_i \cap \widehat{\mathcal{E}}_i|) = |\widetilde{\mathcal{E}}_i|\frac{|\widehat{\mathcal{E}}_i|}{|\mathcal{V}|} = K\frac{|\widehat{\mathcal{E}}_i|}{|\mathcal{V}|}$. □

Furthermore, we present Theorem 3 to state the relationships between the LP performance under each evaluation metric and the node degree:

Theorem 3. *Given that $|\widetilde{\mathcal{E}}_i \cap \widehat{\mathcal{E}}_i|$ follows hyper-geometric distribution, we have:*

$$E(\mathrm{R@}K_i|d) = \frac{K}{N}, \frac{\partial E(\mathrm{R@}K|d)}{\partial d} = 0, \tag{12}$$

$$E(\mathrm{P@}K|d_i) = \frac{\alpha d}{N}, \frac{\partial E(\mathrm{P@}K|d)}{\partial d} = \frac{\alpha}{N}, \tag{13}$$

$$E(\mathrm{F1@}K|d) = \frac{2K}{N}\frac{\alpha d}{K+\alpha d}, \frac{\partial E(\mathrm{F1@}K|d)}{\partial d} = \frac{2\alpha K^2}{N}\frac{1}{(K+\alpha d)^2}, \tag{14}$$

$$E(\mathrm{N@}K|d) = \frac{\alpha d}{N}, \frac{\partial E(\mathrm{N@}K|d)}{\partial d} = \frac{\alpha}{N}. \tag{15}$$

Proof.

$$E(\mathrm{R@}K_i|d) = E(\frac{|\widetilde{\mathcal{E}}_i \cap \widehat{\mathcal{E}}_i|}{|\widehat{\mathcal{E}}_i|}) = \frac{E(|\widetilde{\mathcal{E}}_i \cap \widehat{\mathcal{E}}_i|)}{|\widehat{\mathcal{E}}_i|} = \frac{\frac{|\widehat{\mathcal{E}}_i|}{|\mathcal{V}|}K}{|\widehat{\mathcal{E}}_i|} = \frac{K}{N} \tag{16}$$

$$E(\mathrm{P@}K_i|d) = E(\frac{|\widetilde{\mathcal{E}}_i \cap \widehat{\mathcal{E}}_i|}{K}) = \frac{E(|\widetilde{\mathcal{E}}_i \cap \widehat{\mathcal{E}}_i|)}{K} = \frac{\frac{|\widehat{\mathcal{E}}_i|}{|\mathcal{V}|}K}{K} = \frac{\alpha d}{N} \tag{17}$$

$$E(\mathrm{F1@}K_i|d) = E(\frac{2|\widetilde{\mathcal{E}}_i \cap \widehat{\mathcal{E}}_i|}{K+|\widehat{\mathcal{E}}_i|}) = \frac{2E(|\widetilde{\mathcal{E}}_i \cap \widehat{\mathcal{E}}_i|)}{K+\alpha d} = \frac{2K}{N}\frac{\alpha d}{K+\alpha d} \tag{18}$$

$$E(\mathrm{N@}K_i|d) = E(\frac{\sum_{k=1}^K \frac{\mathbb{1}[v_{\phi^k} \in (\widetilde{\mathcal{E}}_i \cap \widehat{\mathcal{E}}_i)]}{\log_2(k+1)}}{\sum_{k=1}^K \log_2(k+1)}) = \frac{E(\sum_{k=1}^K \frac{\mathbb{1}[v_{\phi^k} \in (\widetilde{\mathcal{E}}_i \cap \widehat{\mathcal{E}}_i)]}{\log_2(k+1)})}{\sum_{k=1}^K \frac{1}{\log_2(k+1)}} \tag{19}$$

To calculate the numerator DCG, i.e., $E(\sum_{k=1}^K \frac{\mathbb{1}[v_{\phi^k} \in (\widetilde{\mathcal{E}}_i \cap \widehat{\mathcal{E}}_i)]}{\log_2(k+1)})$ in Eq. (19), we model the link prediction procedure as 1) randomly select K nodes from the whole node space $\mathcal{V}$; 2) calculate $|\widetilde{\mathcal{E}}_i \cap \widehat{\mathcal{E}}_i|$, i.e., how many nodes among the selected nodes $\widetilde{\mathcal{E}}_i$ are in the ground-truth neighborhood list $\widehat{\mathcal{E}}_i$; 3) randomly select $|\widetilde{\mathcal{E}}_i \cap \widehat{\mathcal{E}}_i|$ slots to position nodes in $\widetilde{\mathcal{E}}_i \cap \widehat{\mathcal{E}}_i$ and calculate DCG. The above steps can be mathematically formulated as:

$$\sum_{i=0}^K \frac{C(N-\alpha d, K-i)C(\alpha d, i)}{C(N,K)} \sum_{j=1}^{C(K,i)} p(\mathbf{O}_j^{(K,i)}) \sum_{k=1}^K \frac{\mathbb{1}[\mathbf{O}_{jk}^{(K,i)} = 1]}{\log_2(k+1)}, \tag{20}$$

where $\mathbf{O}^{(K,i)} \in \{0,1\}^{C(K,i)\times K}$ represents all $C(K,i)$ possible positional indices of putting i nodes into K candidate slots. Specifically $\mathbf{O}_j^{(K,i)} \in \{0,1\}^K$ indicates the j^{th} positional configuration of i nodes where $\mathbf{O}_{jk}^{(K,i)} = 1$ if an node is positioned at k^{th} slot and $\mathbf{O}_{jk}^{(K,i)} = 0$ otherwise. Since our link predictor has no bias in positioning nodes in the K slots by Lemma 1, we have $p(\mathbf{O}_j^{(K,i)}) = \frac{1}{C(K,i)}$ and Eq. (20) can be transformed as:

$$\sum_{i=0}^{K} \frac{C(N-\alpha d, K-i)C(\alpha d, i)}{C(N,K)} \frac{1}{C(K,i)} \sum_{j=1}^{C(K,i)} \sum_{k=1}^{K} \frac{\mathbb{1}[\mathbf{O}_{jk}^{(K,i)} = 1]}{\log_2(k+1)}. \tag{21}$$

We know that only when the k^{th} slot is positioned a node can we have $\mathbf{O}_{jk}^{(K,i)} = 1$ and among the total $C(K,i)$ selections, every candidate slot $k \in \{1,2,...,K\}$ would be selected $C(K-1,i-1)$ times to position a node, which hence leads to:

$$\sum_{j=1}^{C(K,i)} \sum_{k=1}^{K} \frac{\mathbb{1}[\mathbf{O}_{jk}^{(K,i)} = 1]}{\log_2(k+1)} = \sum_{k=1}^{K} \frac{C(K-1,i-1)}{\log_2(k+1)}. \tag{22}$$

We then substitute Eq. (22) into Eq. (21) as:

$$\begin{aligned} &\sum_{i=0}^{K} \frac{C(N-\alpha d, K-i)C(\alpha d, i)}{C(N,K)} \frac{1}{C(K,i)} \sum_{k=1}^{K} \frac{C(K-1,i-1)}{\log_2(k+1)} \\ &= \sum_{i=0}^{K} \frac{C(N-\alpha d, K-i)C(\alpha d, i)}{C(N,K)} \frac{C(K-1,i-1)}{C(K,i)} \sum_{k=1}^{K} \frac{1}{\log_2(k+1)}. \end{aligned} \tag{23}$$

Further substituting Eq. (23) into Eq. (19), we finally get:

$$\begin{aligned} E(\text{N@}K|d_i) &= \sum_{i=0}^{K} \frac{C(N-\alpha d, K-i)C(\alpha d, i)}{C(N,K)} \frac{C(K-1,i-1)}{C(K,i)} \\ &= \sum_{i=0}^{K} \frac{C(N-\alpha d, K-i)C(\alpha d, i)}{C(N,K)} \frac{\frac{(K-1)!}{(i-1)!(K-i)!}}{\frac{K!}{i!(K-i)!}} \\ &= \frac{1}{K} \underbrace{\sum_{i=0}^{K} i \frac{C(N-\alpha d, K-i)C(\alpha d, i)}{C(N,K)}}_{E(|\widetilde{\mathcal{E}}_i \cap \widehat{\mathcal{E}}_i|)} = \frac{1}{K}\frac{\alpha d}{N} * K = \frac{\alpha d}{N} \end{aligned} \tag{24}$$

□

Based on Theorem 3, Precision, F1, and NDCG increase as node degree increases even when no observed links are used to train the link predictor, which informs the degree-related evaluation bias and causes the illusion that high-degree nodes are more advantageous than low-degree ones observed in some previous works (Li et al., 2021; Rahmani et al., 2022).

D.3 Reweighting by LP Score Enhance 1-layer TC

Theorem 4. *Taking the normalization term $g(|\mathcal{H}_i^1|, |\mathcal{H}_j^1|) = |\mathcal{H}_i^1|$ and also assume that higher link prediction score $\mathbf{S}_{ij}$ between v_i and its neighbor v_j corresponds to more number of connections between v_j and the neighborhood $\mathcal{N}_i^{\text{Train}}$, i.e., $\mathbf{S}_{ij} > \mathbf{S}_{ik} \rightarrow |\mathcal{N}_j^{1,\text{Train}} \cap \mathcal{N}_i^{1,\text{Train}}| > |\mathcal{N}_k^{1,\text{Train}} \cap \mathcal{N}_i^{1,\text{Train}}|, \forall v_j, v_k \in \mathcal{N}_i^{\text{Train},1}$, then we have:*

$$\widehat{C}_i^{1,\text{Train}} = \sum_{v_j \sim \mathcal{N}_i^{\text{Train}}} \frac{\mathbf{S}_{ij}|\mathcal{H}_i^1 \cap \mathcal{H}_j^1|}{|\mathcal{H}_i^1|} \geq \mathbb{E}_{v_j \sim \mathcal{N}_i^{\text{Train}}} \frac{|\mathcal{H}_i^1 \cap \mathcal{H}_j^1|}{|\mathcal{H}_i^1|} = C_i^{1,\text{Train}} \tag{25}$$

Proof. By definition, we have $\mathcal{H}_i^1 = \mathcal{N}_i^{1,\text{Train}}$, then the computation of 1-layer TC^{Train} is transformed as:

$$C_i^{1,\text{Train}} = \mathbb{E}_{v_j \sim \mathcal{N}_i^{\text{Train}}} I(\mathcal{S}_i^1, \mathcal{S}_j^1) = \mathbb{E}_{v_j \sim \mathcal{N}_i^{\text{Train}}} \frac{|\mathcal{N}_i^{\text{Train}} \cap \mathcal{N}_j^{\text{Train}}|}{|\mathcal{N}_i^{\text{Train}}|} = \frac{1}{|\mathcal{N}_i^{\text{Train}}|} \mathbb{E}_{v_j \sim \mathcal{N}_i^{\text{Train}}} (|\mathcal{N}_i^{\text{Train}} \cap \mathcal{N}_j^{\text{Train}}|). \tag{26}$$

On the other hand, we similarly transform weighted TC as:

$$\widehat{C}_i^{1,\text{Train}} = \frac{1}{|\mathcal{N}_i^{\text{Train}}|} \sum_{v_j \sim \mathcal{N}_i^{\text{Train}}} (\mathbf{S}_{ij} |\mathcal{N}_i^{\text{Train}} \cap \mathcal{N}_j^{\text{Train}}|). \tag{27}$$

By the relation that:

$$\mathbf{S}_{ij} > \mathbf{S}_{ik} \rightarrow |\mathcal{N}_j^{1,\text{Train}} \cap \mathcal{N}_i^{1,\text{Train}}| > |\mathcal{N}_k^{1,\text{Train}} \cap \mathcal{N}_i^{1,\text{Train}}|, \forall v_j, v_k \in \mathcal{N}_i^{\text{Train},1}, \tag{28}$$

Then we have:

$$\widehat{C}_i^{1,\text{Train}} \geq C_i^{1,\text{Train}} \tag{29}$$

□

Moreover, we include Figure 9 to illustrate the idea of enhancing TC via assigning higher weights to edges connecting neighbors that have higher connections to the whole neighborhoods. We can see in this case, weighted TC in Figure 9(a) is naturally higher than the one in Figure 9(b)

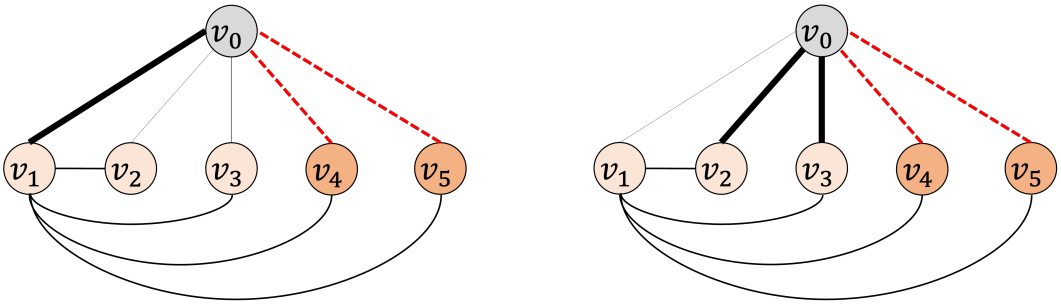

Figure 9: (a) Increasing the weight of neighbors that have more connections with the whole neighborhood while (b) increasing the weight of neighbors that have fewer connections with the whole neighborhood. (a) would increase the weighted TC while (b) would not

E EXAMPLE DEMONSTRATING THE ADVANTAGES OF TC OVER LCC

According to the definition of local clustering coefficient (LCC) and TC, we respectively calculate their values for node v_1 in Figure 10. v_2, v_3, v_4 do not have any connection among themselves, indicating node v_1 prefer interacting with nodes coming from significantly different domain/community. Subsequently, the incoming neighbors v_5, v_6 of v_1 are likely to also come from other communities and hence share no connections with v_2, v_3, v_4, which leads to the ill topological condition for predicting links of v_1. However, in this case, the clustering coefficient still maintains 0.5 because of the connections between v_1 and $v_2/v_3/v_4$, which cannot precisely capture the ill-topology of v_1 in this case. Conversely, our TC^{Train} equals 0, reflecting the ill topological condition of v_1.

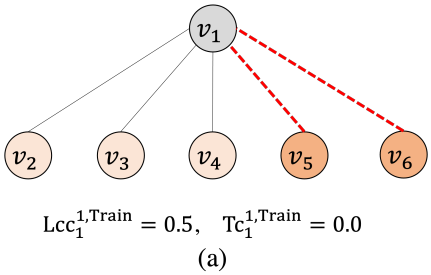

Figure 10: Comparison of TC and LCC

F Datasets and Experimental Settings

This section introduces datasets and experimental settings used in this paper.

F.1 Dataset Introduction and Statistics

We use five widely employed datasets for evaluating the link prediction task, including four citation networks: Cora, Citeseer, Pubmed, and Citation2, and 1 human social network Collab. We further introduce two real-world animal social networks, Reptile and Vole, based on animal interactions.

- **Cora/Citeseer/Pubmed**: Following (Zhao et al., 2022; Chamberlain et al., 2022; Wang et al., 2023), we randomly split edges into 70%/10%/20% so that there is no topological distribution shift in these datasets. We use Hits@100 to evaluate the final performance.
- **Collab/Citation2**: We leverage the default edge splitting from OGBL (Hu et al., 2020). These two datasets mimic the real-life link prediction scenario where testing edges later joined in the network than validation edges and further than training edges. This would cause the topological distribution shift observed in the **Obs.3** of Section 3.3. For Collab, different from (Chamberlain et al., 2022; Wang et al., 2023), our setting does not allow validation edges to join the network for message-passing when evaluating link prediction performance. Therefore, the edges used for message-passing and supervision come from edges in the training set. In addition, we also consider a widely used setting in prior work where the validation edges would be allowed in message-passing when evaluating in the testing stage and we term this one on Collab as Collab* (Wang et al., 2023; Chamberlain et al., 2022).
- **Reptile/Vole**: we obtain the dataset from Network Repository (Rossi & Ahmed, 2015). To construct this network, a bipartite network was first constructed based on burrow use - an edge connecting a tortoise node to a burrow node indicated a burrow used by the individual. Social networks of desert tortoises were then constructed by the bipartite network into a single-mode projection of tortoise nodes. Node features are initialized by a trainable embedding layer, and we leverage the same edge splitting 70%/10%/20% for training/validation/testing.

Table 3: Statistic of datasets used for evaluating link prediction.

Network Domain	Dataset	# Nodes	# Edges	Split Type	Metric	Split Ratio
Citation Network	Cora	2,708	5,278	Random	Hits@100	70/10/20%
	Citeseer	3,327	4,676	Random	Hits@100	70/10/20%
	Pubmed	18,717	44,327	Random	Hits@100	70/10/20%
	Citation2	2,927,963	30,561,187	Time	MRR	Default
Social Network	Collab	235,868	1,285,465	Time	Hits@50	Default
Animal Network	Reptile	787	1232	Random	Hits@100	70/10/20%
	Vole	1480	3935	Random	Hits@100	70/10/20%

F.2 Hyperparameter Details

For all experiments, we select the best configuration on validation edges and report the model performance on testing edges. The search space for the hyperparameters of the GCN/SAGE/LightGCN baselines and their augmented variants GCN$_{rw}$/SAGE$_{rw}$ are: graph convolutional layer $\{1, 2, 3\}$, hidden dimension of graph encoder $\{64, 128, 256\}$, the learning rate of the encoder and predictor $\{0.001, 0.005, 0.01\}$, dropout $\{0.2, 0.5, 0.8\}$, training epoch $\{50, 100, 500, 1000\}$, batch size $\{256, 1152, 64 * 1024\}$ (Hu et al., 2020; Chamberlain et al., 2022; Wang et al., 2023), weights $\alpha \in \{0.5, 1, 2, 3, 4\}$, the update interval $\tau \in \{1, 2, 10, 20, 50\}$, warm up epochs $T^{\text{warm}} \in \{1, 2, 5, 10, 30, 50\}$. For baseline NCN[2], we directly run their code using their default best-performing configurations on Cora/Citeseer/Pubmed/Collab but for Citation2, due to memory limitation, we directly take the result from the original paper. We use cosine similarity metric as the similarity function ϕ in computing ATC.

[2]https://github.com/GraphPKU/NeuralCommonNeighbor

G ADDITIONAL RESULTS

To demonstrate that the observations made previously in Section 3 can also generalize to other datasets, here we present the comprehensive results on all datasets we study in this paper as follows.

G.1 LINK PREDICTION PERFORMANCE GROUPED BY TC^{Test}

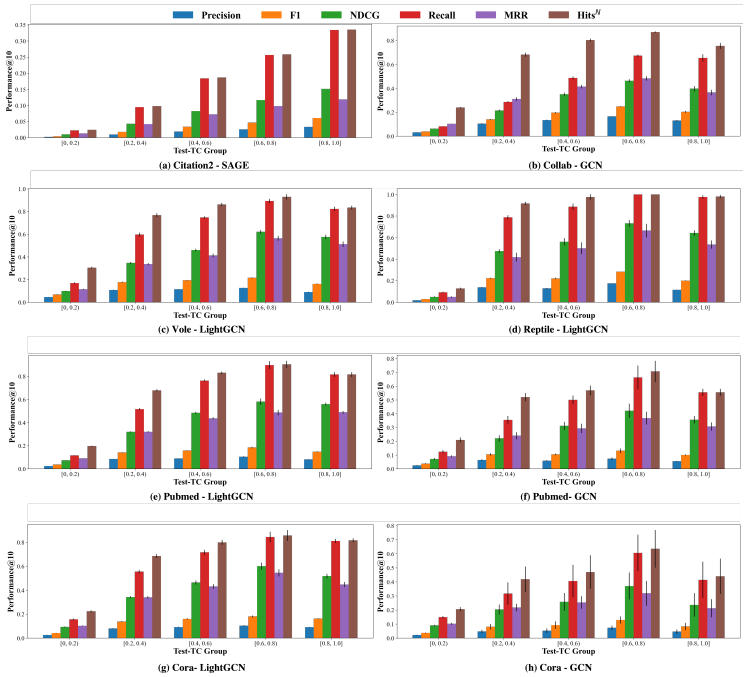

Figure 11: LP performance grouped by TC^{Test} for all nodes

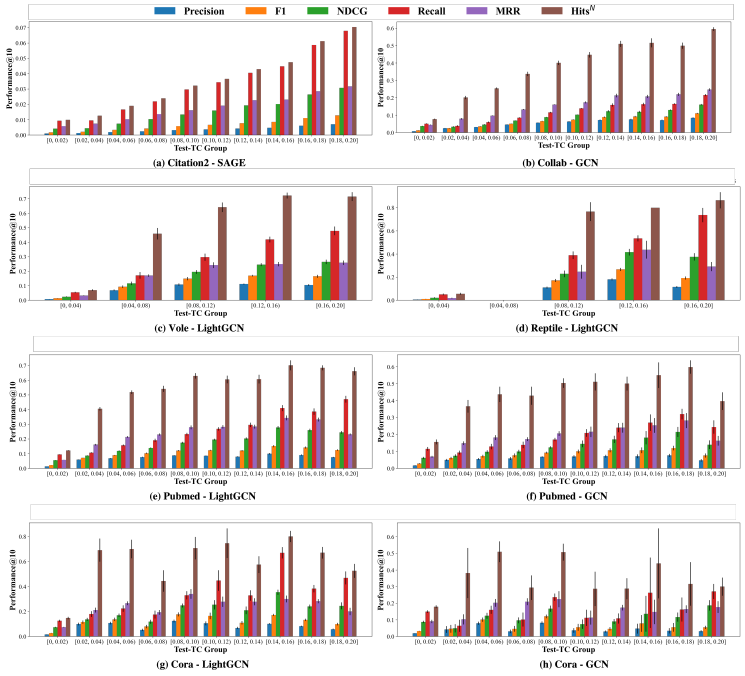

Figure 12: LP performance grouped by TC^{Test} for low TC^{Test} nodes

G.2 LINK PREDICTION PERFORMANCE GROUPED BY TC^{Train}

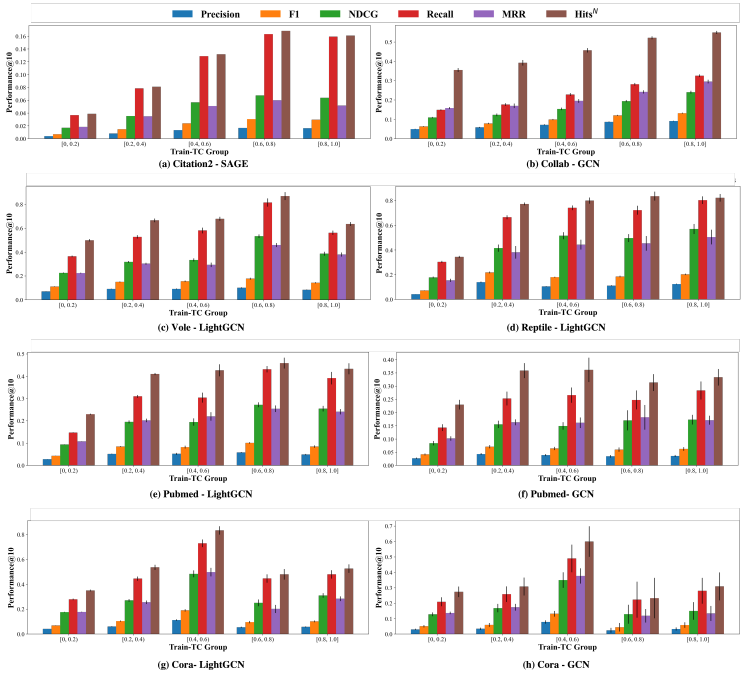

Figure 13: LP performance grouped by TC^{Train} for all nodes

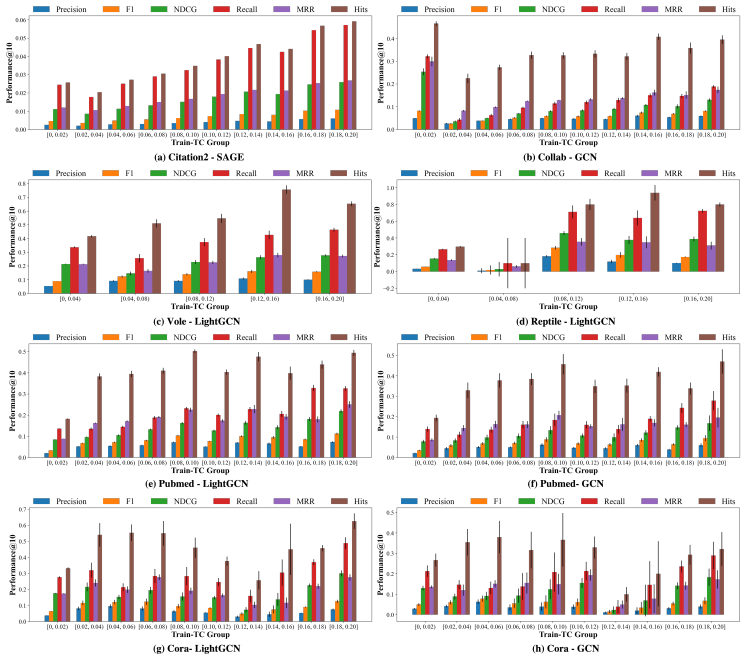

Figure 14: LP performance grouped by TC^{Train} for low TC^{Train} nodes

G.3 LINK PREDICTION PERFORMANCE GROUPED BY DEGREE$^{\text{Test}}$

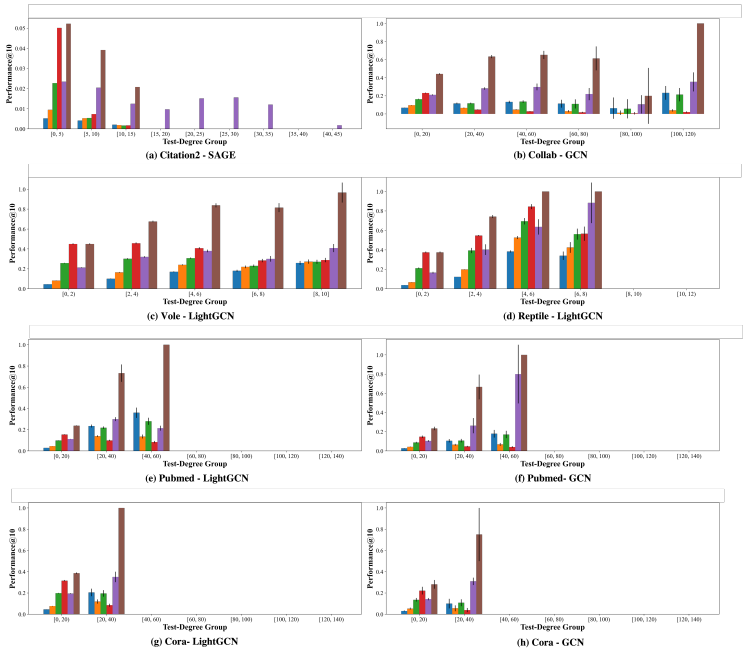

Figure 15: LP performance grouped by Degree$^{\text{Test}}$ for all nodes

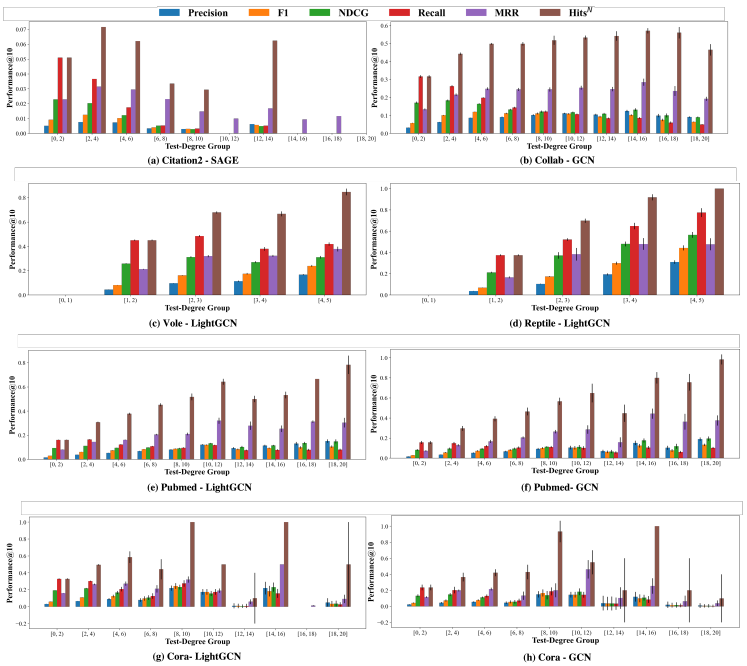

Figure 16: LP performance grouped by Degree$^{\text{Test}}$ for low Test-Degree nodes

G.4 LINK PREDICTION PERFORMANCE GROUPED BY DEGREE$^{\text{Train}}$

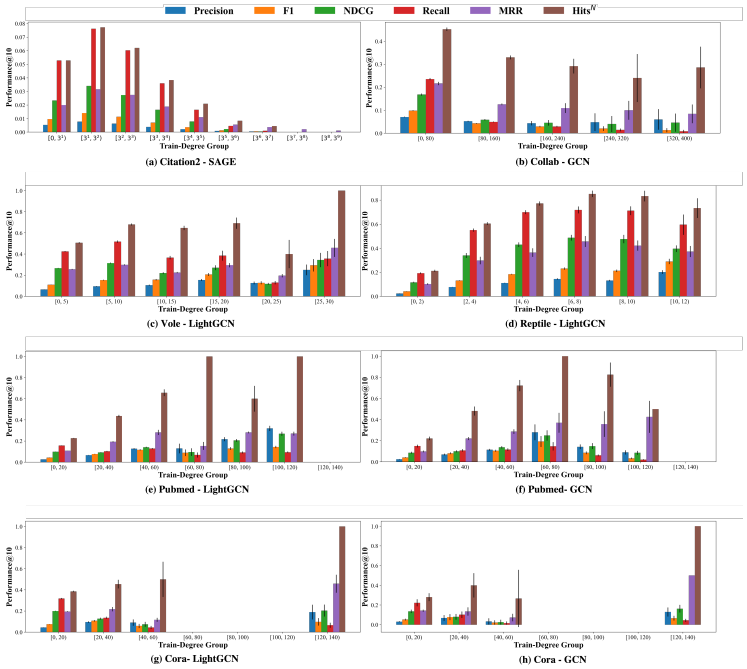

Figure 17: LP performance grouped by Degree$^{\text{Train}}$ for all nodes

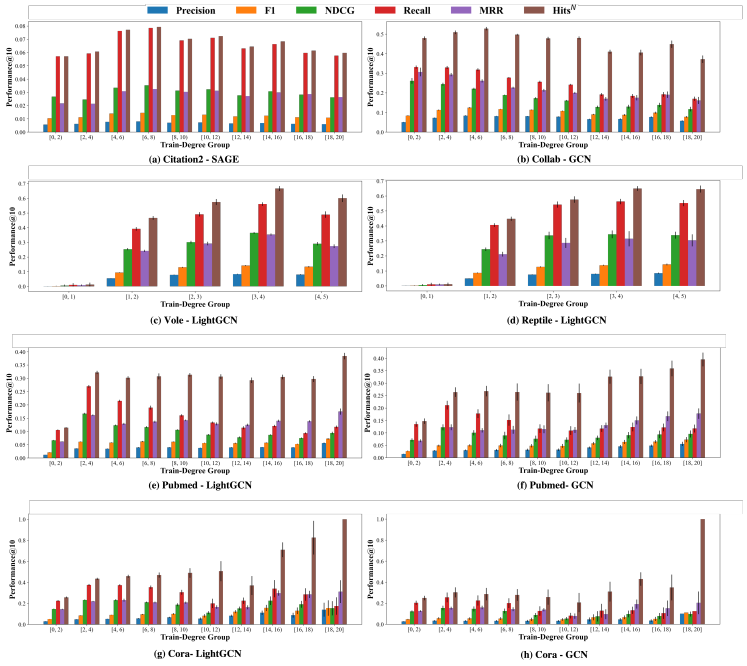

Figure 18: LP performance grouped by Degree$^{\text{Train}}$ for low Degree$^{\text{Train}}$ nodes

G.5 Relation between LP performance and TC at Graph-level

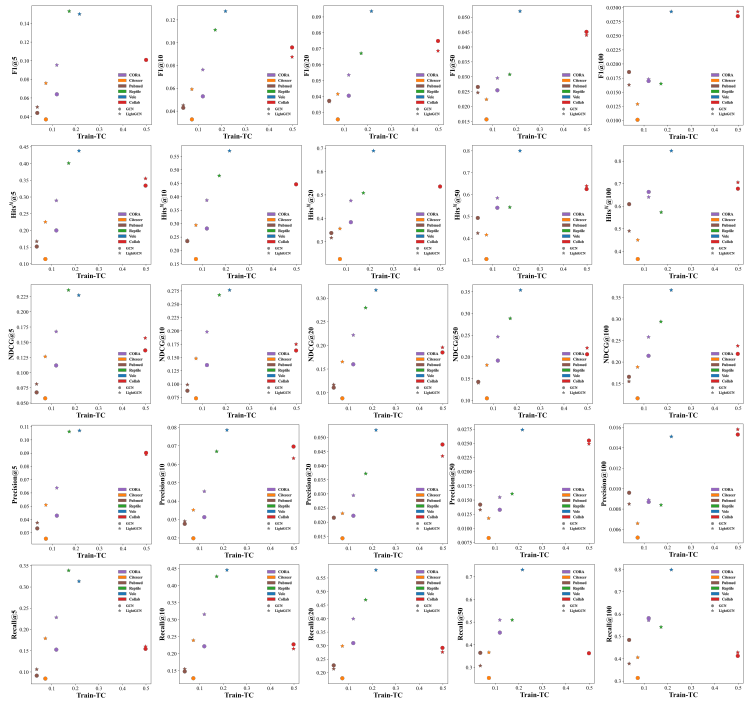

Figure 19: Relation between LP performance and TC at Graph-level

G.6 Relation between TC^{Train} and TC^{Test}

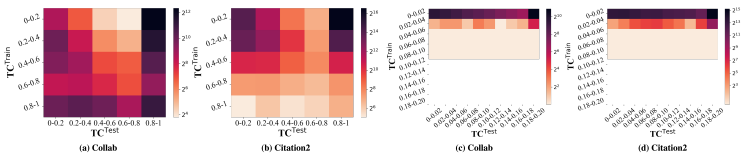

Figure 20: Relation between TC^{Train} and TC^{Test} on Collab/Citation2

G.7 Difference in TC vs Difference in Performance before/after applying reweighting

G.8 Correlation of the performance with TC and Degree

Here we present the comprehensive correlation of the performance with TC^{Train}/TC^{Val}/TC^{Test} and $Degree^{Train}$. As the performance is evaluated under different K, we further define the absolute average/the typical average correlation across different K values to reflect the absolute correlation strength/the consistency of the correlation average:

$$\text{Absolute Avg.}_{X@K} = \frac{1}{4}\sum_{k\in\{5,10,20,50\}} |X@k|, \qquad \text{Basic Avg.}_{X@K} = \frac{1}{4}\sum_{k\in\{5,10,20,50\}} X@k$$

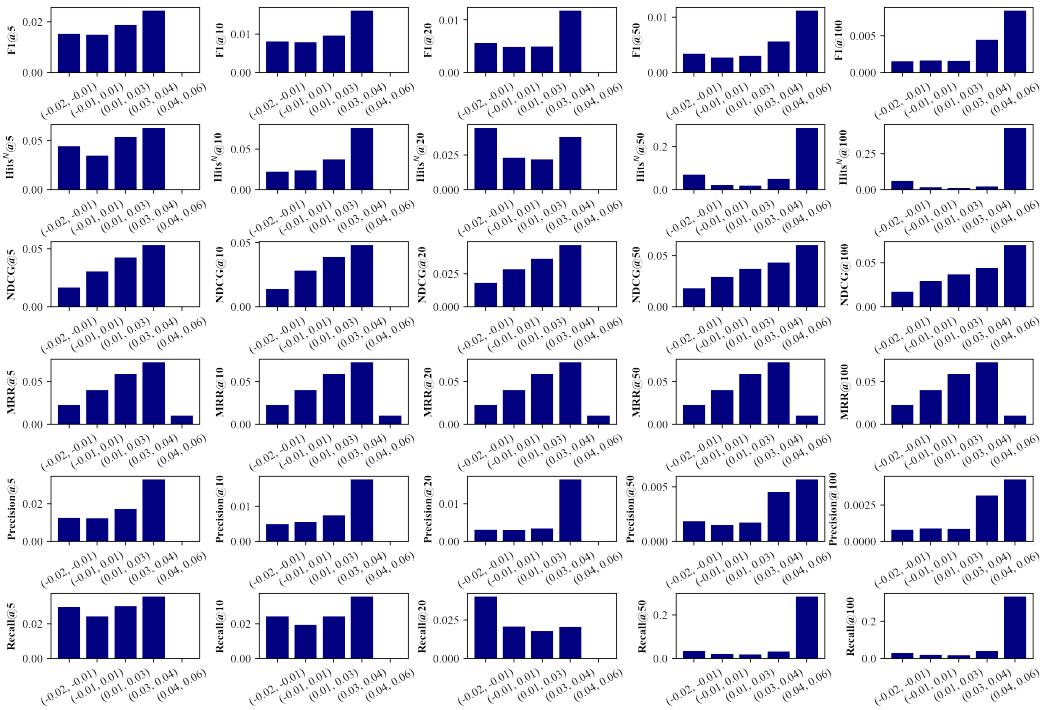

Figure 21: Relation between TC^{Train} and TC^{Test} on Collab by running GCN

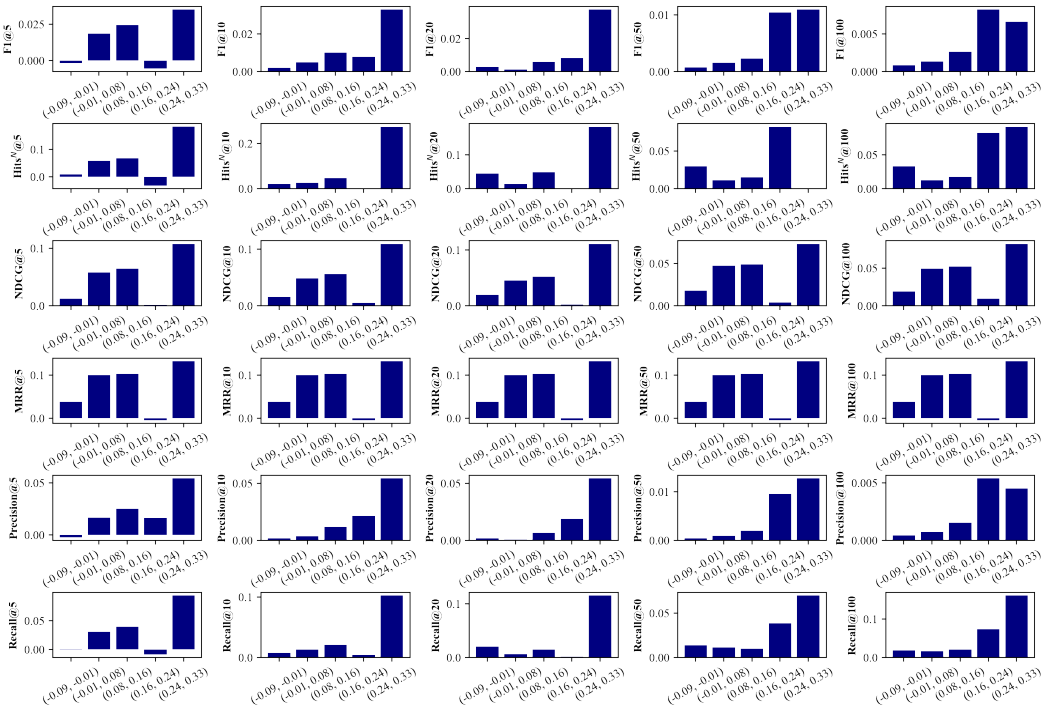

Figure 22: Relation between TC^{Train} and TC^{Test} on Collab by running SAGE

Table 4: The correlation between TC^{Train}/TC^{Val}/TC^{Test}/$Degree^{Train}$ and the GCN's LP performance on **Collab**. We note that the formal definitions of Absolute Avg. and Basic Avg. are provided in Section and they represent the average absolute and simple average correlation, respectively, across the range of @K for the given metric; these are also then calculated overall.

	Metric	@5	@10	@20	@50	Absolute Avg.	Basic Avg.
TC^{Train}	Precision	0.2252	0.1925	0.1353	0.0578	0.1527	0.1527
	F1	0.2601	0.2364	0.1733	0.0790	0.1872	0.1872
	NDCG	0.2279	0.2427	0.2375	0.2206	0.2322	0.2322
	Recall	0.2296	0.2358	0.2156	0.1754	0.2141	0.2141
	$Hits^N$	0.2057	0.1800	0.1328	0.0717	0.1476	0.1476
	MRR			0.2044		0.2044	0.2044
						0.1867	0.1867
TC^{Val}	Precision	0.2573	0.2832	0.2788	0.2387	0.2645	0.2645
	F1	0.2425	0.2901	0.2991	0.2641	0.2740	0.2740
	NDCG	0.2066	0.2330	0.2521	0.2624	0.2385	0.2385
	Recall	0.1742	0.2179	0.2428	0.2514	0.2216	0.2216
	$Hits^N$	0.2445	0.2674	0.2720	0.2620	0.2615	0.2615
	MRR			0.2350		0.2350	0.2350
						0.2520	0.2520
TC^{Test}	Precision	0.5184	0.5437	0.5107	0.4127	0.4964	0.4964
	F1	0.5858	0.6311	0.5964	0.4799	0.5733	0.5733
	NDCG	0.5443	0.6282	0.6706	0.6902	0.6333	0.6333
	Recall	0.5644	0.6753	0.7324	0.7533	0.6814	0.6814
	$Hits^N$	0.5272	0.5816	0.5924	0.5720	0.5683	0.5683
	MRR			0.5085		0.5085	0.5085
						0.5905	0.5905
$Degree^{Train}$	Precision	-0.1261	-0.0829	0.0006	0.1440	0.0884	-0.0161
	F1	-0.1997	-0.1663	-0.0813	0.0812	0.1321	-0.0915
	NDCG	-0.1822	-0.2017	-0.1985	-0.1750	0.1894	-0.1894
	Recall	-0.2183	-0.2288	-0.2118	-0.1681	0.2068	-0.2068
	$Hits^N$	-0.1395	-0.1164	-0.0658	0.0055	0.0818	-0.0791
	MRR			-0.1349		-0.1349	-0.1349
						0.1397	-0.1166
$Degree^{Val}$	Precision	0.0047	0.0472	0.1117	0.2141	0.0944	0.0944
	F1	-0.0823	-0.0469	0.0200	0.1416	0.0727	0.0081
	NDCG	-0.0608	-0.0803	-0.0838	-0.0736	0.0746	-0.0746
	Recall	-0.1203	-0.1296	-0.1269	-0.1100	0.1217	-0.1217
	$Hits^N$	-0.0063	0.0171	0.0481	0.0848	0.0391	0.0359
	MRR			-0.0108		-0.0108	-0.0108
						0.0805	-0.0116
$Degree^{Test}$	Precision	0.1075	0.1833	0.2924	0.4617	0.2612	0.2612
	F1	-0.0669	0.0043	0.1249	0.3375	0.1334	0.1000
	NDCG	-0.034	-0.0723	-0.0814	-0.0668	0.0636	-0.0636
	Recall	-0.1678	-0.1856	-0.187	-0.1724	0.1782	-0.1782
	$Hits^N$	0.0785	0.1103	0.1407	0.1718	0.1253	0.1253
	MRR			0.0727		0.0727	0.0727
						0.1524	0.0489
Subgraph Density	Precision	0.2199	0.1646	0.0875	-0.0073	0.1198	0.1162
	F1	0.2806	0.2259	0.1353	0.0161	0.1645	0.1645
	NDCG	0.2811	0.2891	0.2748	0.2491	0.2735	0.2735
	Recall	0.2911	0.2783	0.2399	0.1834	0.2482	0.2482
	$Hits^N$	0.2265	0.1842	0.1196	0.0423	0.1432	0.1432
	MRR			0.2331		0.2331	0.2331
						0.1898	0.1891

Table 5: The correlation between TC^{Train}/TC^{Val}/TC^{Test}/$Degree^{Train}$ and the GCN's LP performance on **Citation2**. We note that the formal definitions of Absolute Avg. and Basic Avg. are provided in Section and they represent the average absolute and simple average correlation, respectively, across the range of @K for the given metric; these are also then calculated overall.

	Metric	@5	@10	@20	@50	Absolute Avg.	Basic Avg.
TC^{Train}	Precision	0.0839	0.1312	0.1784	0.2157	0.1523	0.1523
	F1	0.0849	0.1323	0.1795	0.2165	0.1533	0.1533
	NDCG	0.0773	0.1164	0.1585	0.2012	0.1384	0.1384
	Recall	0.0860	0.1346	0.1845	0.2265	0.1579	0.1579
	$Hits^N$	0.0840	0.1314	0.1791	0.2182	0.1532	0.1532
	MRR			0.1229		0.1229	0.1229
						0.1510	0.1510
TC^{Val}	Precision	0.0575	0.0868	0.1200	0.1479	0.1031	0.1031
	F1	0.0581	0.0874	0.1206	0.1484	0.1036	0.1036
	NDCG	0.0545	0.0790	0.1078	0.1377	0.0948	0.0948
	Recall	0.0586	0.0884	0.1231	0.1540	0.1060	0.1060
	$Hits^N$	0.0574	0.0870	0.1206	0.1500	0.1038	0.1038
	MRR			0.0846		0.0846	0.0846
						0.1022	0.1022
TC^{Test}	Precision	0.1797	0.2541	0.3313	0.3996	0.2912	0.2912
	F1	0.1812	0.2558	0.3328	0.4008	0.2927	0.2927
	NDCG	0.1706	0.2365	0.3071	0.3825	0.2742	0.2742
	Recall	0.1829	0.2599	0.3401	0.4141	0.2993	0.2993
	$Hits^N$	0.1797	0.2550	0.3331	0.4048	0.2932	0.2932
	MRR			0.2512		0.2512	0.2512
						0.2901	0.2901
$Degree^{Train}$	Precision	-0.0288	-0.0406	-0.0536	-0.0689	0.0480	-0.0480
	F1	-0.0295	-0.0415	-0.0546	-0.0699	0.0489	-0.0489
	NDCG	-0.0285	-0.0394	-0.0522	-0.0692	0.0473	-0.0473
	Recall	-0.0305	-0.0436	-0.0589	-0.0791	0.0530	-0.0530
	$Hits^N$	-0.0289	-0.0408	-0.0540	-0.0708	0.0486	-0.0486
	MRR			-0.0421		-0.0421	-0.0421
						0.0492	0.0492
$Degree^{Val}$	Precision	0.0161	0.0229	0.0300	0.0393	0.0271	0.0271
	F1	0.0156	0.0220	0.0289	0.0381	0.0262	0.0262
	NDCG	0.0150	0.0199	0.0248	0.0305	0.0226	0.0226
	Recall	0.0150	0.0203	0.0252	0.0301	0.0227	0.0227
	$Hits^N$	0.0161	0.0232	0.0300	0.0384	0.0269	0.0269
	MRR			0.0234		0.0234	0.0234
						0.0251	0.0251
$Degree^{Test}$	Precision	0.0060	0.0113	0.0190	0.0364	0.0182	0.0182
	F1	-0.0009	0.0047	0.0128	0.0314	0.0125	0.0120
	NDCG	-0.0086	-0.0113	-0.0147	-0.0185	0.0133	-0.0133
	Recall	-0.0135	-0.0185	-0.0251	-0.0344	0.0229	-0.0229
	$Hits^N$	0.0051	0.0081	0.0120	0.0159	0.0103	0.0103
	MRR			0.0104		0.0104	0.0104
						0.0154	0.0009
Subgraph Density	Precision	0.0809	0.1217	0.1607	0.1916	0.1387	0.1387
	F1	0.0823	0.1231	0.1621	0.1926	0.1400	0.1400
	NDCG	0.0761	0.1111	0.1476	0.1853	0.1300	0.1300
	Recall	0.0842	0.1268	0.1691	0.2063	0.1466	0.1466
	$Hits^N$	0.0811	0.1219	0.1618	0.1956	0.1401	0.1401
	MRR			0.1144		0.1144	0.1144
						0.1391	0.1391

Table 6: The correlation between TC^{Train}/TC^{Val}/TC^{Test}/$Degree^{Train}$ and the GCN's LP performance on **Cora**. We note that the formal definitions of Absolute Avg. and Basic Avg. are provided in Section and they represent the average absolute and simple average correlation, respectively, across the range of @K for the given metric; these are also then calculated overall.

	Metric	@5	@10	@20	@50	Absolute Avg.	Basic Avg.
TC^{Train}	Precision	0.0985	0.1046	0.1238	0.1571	0.1210	0.1210
	F1	0.0989	0.1042	0.1239	0.1597	0.1217	0.1217
	NDCG	0.0933	0.0990	0.1088	0.1306	0.1079	0.1079
	Recall	0.1020	0.1042	0.1162	0.1568	0.1198	0.1198
	$Hits^N$	0.0961	0.1000	0.1226	0.1617	0.1201	0.1201
	MRR			0.0869		0.0869	0.0869
						0.1181	0.1181
TC^{Val}	Precision	0.0342	0.0456	0.0840	0.0903	0.0635	0.0635
	F1	0.0296	0.0406	0.0820	0.0907	0.0607	0.0607
	NDCG	0.0215	0.0259	0.0446	0.0526	0.0362	0.0362
	Recall	0.0257	0.0322	0.0724	0.0841	0.0536	0.0536
	$Hits^N$	0.0331	0.0413	0.0742	0.0932	0.0605	0.0605
	MRR			0.0291		0.0291	0.0291
						0.0549	0.0549
TC^{Test}	Precision	0.4694	0.4702	0.4667	0.3977	0.4510	0.4510
	F1	0.4952	0.4964	0.4948	0.4216	0.4770	0.4770
	NDCG	0.4970	0.5239	0.5551	0.5759	0.5380	0.5380
	Recall	0.4941	0.5109	0.5448	0.5347	0.5211	0.5211
	$Hits^N$	0.4749	0.4909	0.5130	0.4866	0.4914	0.4914
	MRR			0.4920		0.4920	0.4920
						0.4957	0.4957
$Degree^{Train}$	Precision	0.0751	0.0970	0.1701	0.3268	0.1673	0.1673
	F1	-0.0039	0.0237	0.0938	0.2549	0.0941	0.0921
	NDCG	-0.0156	-0.0276	-0.0283	-0.0191	0.0227	-0.0227
	Recall	-0.0432	-0.0547	-0.0568	-0.0529	0.0519	-0.0519
	$Hits^N$	0.0656	0.0650	0.0862	0.1135	0.0826	0.0826
	MRR			0.0307		0.0307	0.0307
						0.0837	0.0837
$Degree^{Val}$	Precision	0.0433	0.0623	0.1138	0.2248	0.1111	0.1111
	F1	-0.0230	0.0012	0.0508	0.1634	0.0596	0.0481
	NDCG	-0.0235	-0.0336	-0.0369	-0.0361	0.0325	-0.0325
	Recall	-0.0570	-0.0648	-0.0689	-0.0784	0.0673	-0.0673
	$Hits^N$	0.0253	0.0222	0.0308	0.0431	0.0304	0.0304
	MRR			0.0144		0.0144	0.0144
						0.0602	0.0179
$Degree^{Test}$	Precision	0.1669	0.2104	0.3046	0.4890	0.2927	0.2927
	F1	0.0537	0.1111	0.2127	0.4149	0.1981	0.1981
	NDCG	0.0004	-0.0104	-0.0082	0.0060	0.0063	-0.0031
	Recall	-0.0599	-0.0702	-0.0760	-0.0781	0.0711	-0.0711
	$Hits^N$	0.1406	0.1487	0.1624	0.1865	0.1596	0.1596
	MRR			0.1116		0.1116	0.1116
						0.1455	0.1153
Subgraph Density	Precision	0.0794	0.0900	0.0796	0.0381	0.0718	0.0718
	F1	0.1088	0.1189	0.1066	0.0580	0.0981	0.0981
	NDCG	0.1157	0.1378	0.1543	0.1674	0.1438	0.1438
	Recall	0.1330	0.1690	0.2015	0.2272	0.1827	0.1827
	$Hits^N$	0.0851	0.1109	0.1257	0.1385	0.1151	0.1151
	MRR			0.0976		0.0976	0.0976
						0.1223	0.1223

Table 7: The correlation between TC^{Train}/TC^{Val}/TC^{Test}/$Degree^{Train}$ and the GCN's LP performance on **Citeseer**. We note that the formal definitions of Absolute Avg. and Basic Avg. are provided in Section and they represent the average absolute and simple average correlation, respectively, across the range of @K for the given metric; these are also then calculated overall.

	Metric	@5	@10	@20	@50	Absolute Avg.	Basic Avg.
TC^{Train}	Precision	0.3330	0.3735	0.3898	0.3830	0.3698	0.3698
	F1	0.3324	0.3803	0.4056	0.4049	0.3808	0.3808
	NDCG	0.2831	0.3226	0.3570	0.3879	0.3377	0.3377
	Recall	0.3001	0.3481	0.3920	0.4295	0.3674	0.3674
	$Hits^N$	0.3386	0.3901	0.4287	0.4603	0.4044	0.4044
	MRR			0.3194		0.3194	0.3194
						0.3720	0.3720
TC^{Val}	Precision	0.2796	0.2962	0.3224	0.3229	0.3053	0.3053
	F1	0.2756	0.2947	0.3291	0.3365	0.3090	0.3090
	NDCG	0.2508	0.2662	0.2929	0.3118	0.2804	0.2804
	Recall	0.2491	0.2585	0.2928	0.3086	0.2773	0.2773
	$Hits^N$	0.2801	0.3049	0.338	0.3496	0.3182	0.3182
	MRR			0.2763		0.2763	0.2763
						0.2980	0.2980
TC^{Test}	Precision	0.6786	0.698	0.6745	0.6220	0.6683	0.6683
	F1	0.7157	0.7385	0.7207	0.6678	0.7107	0.7107
	NDCG	0.7037	0.7540	0.7946	0.8300	0.7706	0.7706
	Recall	0.7299	0.7797	0.8258	0.8588	0.7986	0.7986
	$Hits^N$	0.7127	0.7595	0.7979	0.8216	0.7729	0.7729
	MRR			0.7070		0.7070	0.7070
						0.7442	0.7442
$Degree^{Train}$	Precision	0.2472	0.3523	0.4591	0.5861	0.4112	0.4112
	F1	0.1867	0.2727	0.3872	0.5408	0.3469	0.3469
	NDCG	0.1303	0.1645	0.2022	0.2475	0.1861	0.1861
	Recall	0.1144	0.1532	0.2047	0.2591	0.1829	0.1829
	$Hits^N$	0.2538	0.3181	0.3581	0.3886	0.3297	0.3297
	MRR			0.2227		0.2227	0.2227
						0.2913	0.2913
$Degree^{Val}$	Precision	0.1431	0.1866	0.2255	0.277	0.2081	0.2081
	F1	0.1147	0.1582	0.2053	0.2693	0.1869	0.1869
	NDCG	0.0845	0.1014	0.1194	0.1429	0.1121	0.1121
	Recall	0.0693	0.0880	0.1113	0.1411	0.1024	0.1024
	$Hits^N$	0.1438	0.1683	0.1857	0.2148	0.1782	0.1782
	MRR			0.1366		0.1366	0.1366
						0.1575	0.1575
$Degree^{Test}$	Precision	0.3052	0.4412	0.5704	0.7223	0.5098	0.5098
	F1	0.1919	0.3133	0.4639	0.6597	0.4072	0.4072
	NDCG	0.0949	0.1220	0.1548	0.1975	0.1423	0.1423
	Recall	0.0323	0.0562	0.0909	0.1314	0.0777	0.0777
	$Hits^N$	0.2745	0.3258	0.3378	0.3369	0.3188	0.3188
	MRR			0.2444		0.2444	0.2444
						0.2911	0.2911
Subgraph Density	Precision	0.1559	0.1412	0.1168	0.0858	0.1249	0.1249
	F1	0.1867	0.1699	0.1420	0.1035	0.1505	0.1505
	NDCG	0.2006	0.2097	0.2176	0.2235	0.2129	0.2129
	Recall	0.2218	0.2289	0.2411	0.2491	0.2352	0.2352
	$Hits^N$	0.1768	0.1799	0.1982	0.2097	0.1912	0.1912
	MRR			0.1759		0.1759	0.1759
						0.1829	0.1829

Table 8: The correlation between TC^{Train}/TC^{Val}/TC^{Test}/$Degree^{Train}$ and the GCN's LP performance on **Pubmed**. We note that the formal definitions of Absolute Avg. and Basic Avg. are provided in Section and they represent the average absolute and simple average correlation, respectively, across the range of @K for the given metric; these are also then calculated overall.

	Metric	@5	@10	@20	@50	Absolute Avg.	Basic Avg.
TC^{Train}	Precision	0.1981	0.2358	0.2681	0.2924	0.2486	0.2486
	F1	0.1690	0.2216	0.2652	0.2961	0.2380	0.2380
	NDCG	0.1195	0.1379	0.1600	0.1831	0.1501	0.1501
	Recall	0.0917	0.1142	0.1336	0.1397	0.1198	0.1198
	$Hits^N$	0.1932	0.2267	0.2485	0.2513	0.2299	0.2299
	MRR			0.1920		0.1920	0.1920
						0.1973	0.1973
TC^{Val}	Precision	0.1769	0.2180	0.2653	0.3134	0.2434	0.2434
	F1	0.1253	0.1815	0.2462	0.3092	0.2156	0.2156
	NDCG	0.0780	0.0846	0.1046	0.1303	0.0994	0.0994
	Recall	0.0417	0.0503	0.0672	0.0804	0.0599	0.0599
	$Hits^N$	0.1627	0.1882	0.2068	0.2077	0.1914	0.1914
	MRR			0.1607		0.1607	0.1607
						0.1619	0.1619
TC^{Test}	Precision	0.3769	0.3989	0.4078	0.3909	0.3936	0.3936
	F1	0.4011	0.4258	0.4329	0.4088	0.4172	0.4172
	NDCG	0.3902	0.4231	0.4547	0.4870	0.4388	0.4388
	Recall	0.3809	0.4080	0.4286	0.4335	0.4128	0.4128
	$Hits^N$	0.3923	0.4247	0.4463	0.4436	0.4267	0.4267
	MRR			0.4097		0.4097	0.4097
						0.4178	0.4178
$Degree^{Train}$	Precision	0.2433	0.3108	0.3761	0.4849	0.3538	0.3538
	F1	0.1019	0.1970	0.2987	0.4456	0.2608	0.2608
	NDCG	0.0477	0.0366	0.0441	0.0715	0.0500	0.0500
	Recall	-0.0402	-0.0386	-0.0385	-0.0357	0.0383	-0.0383
	$Hits^N$	0.2080	0.2404	0.2504	0.2612	0.2400	0.2400
	MRR			0.2051		0.2051	0.2051
						0.1886	0.1733
$Degree^{Val}$	Precision	0.1823	0.2290	0.2849	0.3681	0.2661	0.2661
	F1	0.0676	0.1368	0.2220	0.3359	0.1906	0.1906
	NDCG	0.0293	0.0164	0.0221	0.0407	0.0271	0.0271
	Recall	-0.0429	-0.0466	-0.0459	-0.0476	0.0458	-0.0458
	$Hits^N$	0.1536	0.1749	0.1831	0.1872	0.1747	0.1747
	MRR			0.1573		0.1573	0.1573
						0.1408	0.1225
$Degree^{Test}$	Precision	0.3073	0.3898	0.4719	0.6133	0.4456	0.4456
	F1	0.1251	0.2423	0.3716	0.5624	0.3254	0.3254
	NDCG	0.0588	0.0406	0.0480	0.0821	0.0574	0.0574
	Recall	-0.0537	-0.0565	-0.0605	-0.0575	0.0571	-0.0571
	$Hits^N$	0.2615	0.2966	0.3030	0.3099	0.2928	0.2928
	MRR			0.2556		0.2556	0.2556
						0.2356	0.2128
Subgraph Density	Precision	0.1002	0.0746	0.0414	-0.0146	0.0577	0.0504
	F1	0.1732	0.1319	0.0792	0.0030	0.0968	0.0968
	NDCG	0.2146	0.2307	0.2357	0.2344	0.2289	0.2289
	Recall	0.2475	0.2547	0.2540	0.2428	0.2498	0.2498
	$Hits^N$	0.1343	0.1330	0.1338	0.1288	0.1325	0.1325
	MRR			0.1430		0.1430	0.1430
						0.1531	0.1517

Table 9: The correlation between TC^{Train}/TC^{Val}/TC^{Test}/$Degree^{Train}$ and the GCN's LP performance on **Vole**. We note that the formal definitions of Absolute Avg. and Basic Avg. are provided in Section and they represent the average absolute and simple average correlation, respectively, across the range of @K for the given metric; these are also then calculated overall.

	Metric	@5	@10	@20	@50	Absolute Avg.	Basic Avg.
TC^{Train}	Precision	0.2725	0.2710	0.2648	0.2287	0.2593	0.2593
	F1	0.2985	0.2981	0.2869	0.2401	0.2809	0.2809
	NDCG	0.2714	0.3012	0.3300	0.3497	0.3131	0.3131
	Recall	0.2946	0.3267	0.3677	0.3917	0.3452	0.3452
	$Hits^N$	0.3113	0.3307	0.3694	0.3988	0.3526	0.3526
	MRR			0.2721		0.2721	0.2721
						0.3102	0.3102
TC^{Val}	Precision	0.1375	0.1717	0.1847	0.1721	0.1665	0.1665
	F1	0.1233	0.1690	0.1871	0.1739	0.1633	0.1633
	NDCG	0.0931	0.1201	0.1403	0.1479	0.1254	0.1254
	Recall	0.0825	0.1251	0.1570	0.1548	0.1299	0.1299
	$Hits^N$	0.1347	0.1558	0.1815	0.1814	0.1634	0.1634
	MRR			0.1219		0.1219	0.1219
						0.1497	0.1497
TC^{Test}	Precision	0.5547	0.4822	0.3937	0.2527	0.4208	0.4208
	F1	0.6498	0.5597	0.4449	0.2742	0.4822	0.4822
	NDCG	0.7395	0.7712	0.7954	0.8030	0.7773	0.7773
	Recall	0.7325	0.7384	0.7367	0.6812	0.7222	0.7222
	$Hits^N$	0.6470	0.6529	0.6452	0.6016	0.6367	0.6367
	MRR			0.6950		0.6950	0.6950
						0.6078	0.6078
$Degree^{Train}$	Precision	0.2103	0.2728	0.3620	0.4508	0.3240	0.3240
	F1	0.1387	0.2253	0.3391	0.4508	0.2885	0.2885
	NDCG	0.0180	0.0352	0.0760	0.1222	0.0629	0.0629
	Recall	0.0238	0.0479	0.1111	0.1993	0.0955	0.0955
	$Hits^N$	0.1688	0.1977	0.2551	0.2989	0.2301	0.2301
	MRR			0.0512		0.0512	0.0512
						0.2002	0.2002
$Degree^{Val}$	Precision	0.0312	0.0747	0.1182	0.1758	0.1000	0.1000
	F1	-0.0135	0.0414	0.0989	0.1685	0.0806	0.0738
	NDCG	-0.0527	-0.0455	-0.0336	-0.0153	0.0368	-0.0368
	Recall	-0.0670	-0.0487	-0.0309	0.0059	0.0381	-0.0352
	$Hits^N$	0.0077	0.0180	0.0368	0.0599	0.0306	0.0306
	MRR			-0.0215		-0.0215	-0.0215
						0.0572	0.0265
$Degree^{Test}$	Precision	0.3731	0.5111	0.6562	0.8126	0.5883	0.5883
	F1	0.2040	0.3944	0.5926	0.7916	0.4957	0.4957
	NDCG	0.0004	0.0257	0.0722	0.1330	0.0578	0.0578
	Recall	-0.0942	-0.0697	-0.0301	0.0419	0.0590	-0.0380
	$Hits^N$	0.2320	0.2604	0.2731	0.2529	0.2546	0.2546
	MRR			0.1642		0.1642	0.1642
						0.2911	0.2717
Subgraph Density	Precision	0.0744	0.0369	-0.0119	-0.0815	0.0512	0.0045
	F1	0.1372	0.0860	0.0187	-0.0689	0.0777	0.0433
	NDCG	0.2205	0.2341	0.2398	0.2398	0.2336	0.2336
	Recall	0.2178	0.2366	0.2495	0.2545	0.2396	0.2396
	$Hits^N$	0.1206	0.1493	0.1688	0.2138	0.1631	0.1631
	MRR			0.2026		0.2026	0.2026
						0.1530	0.1368

Table 10: The correlation between TC^{Train}/TC^{Val}/TC^{Test}/$Degree^{Train}$ and the GCN's LP performance on **Reptile**. We note that the formal definitions of Absolute Avg. and Basic Avg. are provided in Section and they represent the average absolute and simple average correlation, respectively, across the range of @K for the given metric; these are also then calculated overall.

	Metric	@5	@10	@20	@50	Absolute Avg.	Basic Avg.
TC^{Train}	Precision	0.5189	0.5084	0.4977	0.5009	0.5065	0.5065
	F1	0.5420	0.5307	0.5146	0.5090	0.5241	0.5241
	NDCG	0.5298	0.5502	0.5636	0.5741	0.5544	0.5544
	Recall	0.5097	0.5176	0.5343	0.5475	0.5273	0.5273
	$Hits^N$	0.5208	0.5278	0.5407	0.5502	0.5349	0.5349
	MRR			0.5300		0.5300	0.5300
						0.5294	0.5294
TC^{Val}	Precision	0.3994	0.4316	0.4550	0.4647	0.4377	0.4377
	F1	0.3753	0.4250	0.4573	0.4670	0.4312	0.4312
	NDCG	0.3183	0.3535	0.3790	0.3909	0.3604	0.3604
	Recall	0.2670	0.3085	0.3525	0.3744	0.3256	0.3256
	$Hits^N$	0.3213	0.3483	0.3675	0.3840	0.3553	0.3553
	MRR			0.3666		0.3666	0.3666
						0.3820	0.3820
TC^{Test}	Precision	0.7083	0.7000	0.6739	0.6506	0.6832	0.6832
	F1	0.7898	0.7629	0.7138	0.6678	0.7336	0.7336
	NDCG	0.8475	0.8897	0.9029	0.9072	0.8868	0.8868
	Recall	0.8573	0.8858	0.8931	0.8759	0.8780	0.8780
	$Hits^N$	0.8276	0.8566	0.8604	0.8495	0.8485	0.8485
	MRR			0.8163		0.8163	0.8163
						0.8060	0.8060
$Degree^{Train}$	Precision	0.4998	0.5294	0.5664	0.5947	0.5476	0.5476
	F1	0.5082	0.5411	0.5788	0.6017	0.5575	0.5575
	NDCG	0.4247	0.4572	0.4914	0.5120	0.4713	0.4713
	Recall	0.4338	0.4598	0.5201	0.5615	0.4938	0.4938
	$Hits^N$	0.4998	0.5073	0.5391	0.5664	0.5282	0.5282
	MRR			0.4369		0.4369	0.4369
						0.5197	0.5197
$Degree^{Val}$	Precision	0.3185	0.3577	0.3797	0.3924	0.3621	0.3621
	F1	0.3022	0.3546	0.3840	0.3956	0.3591	0.3591
	NDCG	0.2285	0.2617	0.2858	0.2985	0.2686	0.2686
	Recall	0.1997	0.2384	0.2830	0.3093	0.2576	0.2576
	$Hits^N$	0.2729	0.2938	0.3165	0.3339	0.3043	0.3043
	MRR			0.2677		0.2677	0.2677
						0.3103	0.3103
$Degree^{Test}$	Precision	0.6833	0.7492	0.7935	0.8118	0.7595	0.7595
	F1	0.5477	0.6726	0.7556	0.7968	0.6932	0.6932
	NDCG	0.3062	0.3404	0.3676	0.3790	0.3483	0.3483
	Recall	0.1840	0.2103	0.2429	0.2532	0.2226	0.2226
	$Hits^N$	0.3940	0.3555	0.3381	0.3283	0.3540	0.3540
	MRR			0.4468		0.4468	0.4468
						0.4755	0.4755
Subgraph Density	Precision	0.2482	0.2491	0.2211	0.2022	0.2302	0.2302
	F1	0.2943	0.2849	0.2420	0.2108	0.2580	0.2580
	NDCG	0.3560	0.3819	0.3792	0.3765	0.3734	0.3734
	Recall	0.3588	0.3928	0.3777	0.3607	0.3725	0.3725
	$Hits^N$	0.3440	0.3891	0.3837	0.3745	0.3728	0.3728
	MRR			0.3510		0.3510	0.3510
						0.3214	0.3214

H EDGE REWEIGHTING ALGORITHM

Here we present our edge reweigting algorithm to enhance the link prediction performance by modifying the graph adjacency matrix in message-passing. We normalize the adjacency matrix to get $\widetilde{\mathbf{A}}$ and $\widehat{\mathbf{A}}$ as defined in the algorithm below.

Algorithm 1: Edge Reweighting to Boost LP performance

Input: The input training graph $(\mathbf{A}, \mathbf{X}, \mathcal{E}^{\text{Train}}, \mathbf{D})$, graph encoder $f_{\mathbf{\Theta}_f}$, link predictor $g_{\mathbf{\Theta}_g}$, update interval Δ, training epochs T, warm up epochs T^{warm} and weights γ for combining the original adjacency matrix and the updated adjacency matrix. The validation adjacency/degree matrix $\mathbf{A}^{\text{Val}}/\mathbf{D}^{\text{Val}}$ that only includes edges in the validation set.

Compute the normalized adjacency matrices $\widehat{\mathbf{A}} = \mathbf{D}^{-0.5}\mathbf{A}\mathbf{D}^{-0.5}$, $\widetilde{\mathbf{A}} = \mathbf{D}^{-1}\mathbf{A}$, $\widetilde{\mathbf{A}}^{\text{Val}} = \mathbf{D}^{\text{Val}-1}\mathbf{A}^{\text{Val}}$
$\widetilde{\mathbf{A}}^{0} = \widehat{\mathbf{A}}$
for $\tau = 1, \ldots, T$ **do**
  if $\tau \% \Delta \neq 0$ *or* $\tau \leq T^{\text{warm}}$ **then**
    $\widetilde{\mathbf{A}}^{\tau} = \widetilde{\mathbf{A}}^{\tau-1}$
  `/* Message-passing and LP to update model parameters */`
  for *mini-batch of edges* $\mathcal{E}^b \subseteq \mathcal{E}^{\text{Train}}$ **do**
    Sample negative edges $\mathcal{E}^{b,-}$, s.t., $|\mathcal{E}^{b,-}| = |\mathcal{E}^b|$
    Compute node embeddings $\mathbf{H}^{\tau} = f_{\mathbf{\Theta}_f^{\tau-1}}(\widetilde{\mathbf{A}}^{\tau}, \mathbf{X})$
    Compute link prediction scores $\mathbf{E}_{ij}^{\tau} = g_{\mathbf{\Theta}_g^{\tau-1}}(\mathbf{H}_i^{\tau}, \mathbf{H}_j^{\tau}), \forall (i,j) \in \mathcal{E}^b \cup \mathcal{E}^{\text{Train}}$
    $\mathcal{L}^{b,\tau} = -\frac{1}{|\mathcal{E}^b|}(\sum_{e_{ij} \in \mathcal{E}^b} \log \mathbf{E}_{ij}^{\tau} + \sum_{e_{mn} \in \mathcal{E}^{b,-}} \log(1 - \mathbf{E}_{mn}^{\tau}))$
    Update $\mathbf{\Theta}_g^{\tau} \leftarrow \mathbf{\Theta}_g^{\tau-1} - \nabla_{\mathbf{\Theta}_g^{\tau-1}} \mathcal{L}^{b,\tau}$, $\mathbf{\Theta}_f^{\tau} \leftarrow \mathbf{\Theta}_f^{\tau-1} - \nabla_{\mathbf{\Theta}_f^{\tau-1}} \mathcal{L}^{b,\tau-1}$
  `/* Update adjacency matrix to enhance weighted TC */`
  if $\tau \% \Delta == 0$ *and* $\tau > T^{\text{warm}}$ **then**
    Compute node embeddings $\mathbf{H}^{\tau} = f_{\mathbf{\Theta}_f^{\tau-1}}(\widetilde{\mathbf{A}}^{\tau-1}, \mathbf{X})$;
    if *Using training neighbors to reweigh* **then**
      Average pooling the neighborhood embeddings $\mathbf{N}^{\tau} = \widetilde{\mathbf{A}}\mathbf{H}^{\tau}$
    if *Using validation neighbors to reweigh* **then**
      Average pooling the neighborhood embeddings $\mathbf{N}^{\tau} = \widetilde{\mathbf{A}}^{\text{Val}}\mathbf{H}^{\tau}$
    Compute the link prediction scores $\mathbf{S}_{ij}^{\tau} = \frac{\exp(g_{\mathbf{\Theta}_g^{\tau}}(\mathbf{N}_i^{\tau}, \mathbf{H}_j^{\tau}))}{\sum_{j=1}^{n} \exp(g_{\mathbf{\Theta}_g^{\tau}}(\mathbf{N}_i^{\tau}, \mathbf{H}_j^{\tau}))}$
    Update the adjacency matrix $\widetilde{\mathbf{A}}^{\tau} \leftarrow \widehat{\mathbf{A}} + \gamma \mathbf{S}^{\tau}$
Return: $\widetilde{\mathbf{A}}^{\tau}, f_{\mathbf{\Theta}_f^{\tau}}, g_{\mathbf{\Theta}_g^{\tau}}$

I REWEIGH EDGES FOR BASELINES WITHOUT MESSAGE-PASSING

As discussed in Section 4, we enhance node TC^{Train} by reweighing the edges in message-passing. However, for some state-of-the-art baselines Chamberlain et al. (2022) that directly employ the neural transformation rather than message-passing to obtain node embeddings, we reweigh edges in computing the binary cross entropy loss in the training stage as follows:

$$\mathcal{L} = -\frac{1}{|\mathcal{E}^b|} \sum_{e_{ij} \in \mathcal{E}^b} (w_{ij} \sum_{e_{ij} \in \mathcal{E}^b} \log \mathbf{E}_{ij}^{\tau} + w_{mn} \sum_{e_{mn} \in \mathcal{E}^{b,-}} \log(1 - \mathbf{E}_{mn}^{\tau})), \tag{30}$$

where $w_{ij} = \sigma(\phi(\mathbf{N}_i, \mathbf{N}_j))$ quantifies the edge weight between v_i and v_j with σ being the Sigmoid function and ϕ being the cosine similarity. $\mathbf{N}_i$ is the node embedding of v_i obtained in Eq. (2).

Table 11: Comparing the efficiency (s) between X and our proposed X_{rw}.

Baseline	Cora	Citeseer	Pubmed	Collab	Reptile	Vole
GCN	19,5	15.5	158.4	2906	18.3	53.8
GCN_{rw}	21.1	17.2	158.5	2915	17.0	53.0
SAGE	22.3	17.0	189.8	2970	20.9	61.2
$SAGE_{rw}$	23.8	20.5	192.4	2982	21.7	61.9
BUDDY	3.41	4.51	15.51	906.18	2.50	4.99
$BUDDY_{rw}$	3.98	4.92	14.56	907.52	2.62	5.06

J Comparing the Efficiency between Baseline and their Augmented Version by TC

Here we compare the running time (s) of each baseline and their corresponding augmented version by uniformly testing them on the same machine in Table 11. We can see that equipping our proposed reweighting strategy could enhance the performance but only lead to marginal computational overhead. This is because firstly, we only change the weight of existing edges and hence the number of edge weights to be calculated is linear to the network size. Secondly, we leverage the pre-computed node embeddings to compute the edge weights. Thirdly, we only periodically update the edge weights.

K Reweighting Training Neighbors Based on their Connections to Training Neighbors or Validation Neighbors

As discussed in **Obs. 3**, due to the topological distribution shift, the newly joined neighbors of one node become less and less connective to the previous neighbors of that node. Therefore, the training neighbors of one node share fewer connections with the testing neighbors of that node than the validation neighbors. This motivates us to further improve our reweighting strategy based on validation neighbors rather than training neighbors. **The intuition is that when performing message-passing to aggregate training neighbors' information for each node, we want to incorporate those training neighbors with more connections to that node's validation neighbors instead of those training neighbors with more connections to that node's training neighbors.** Technically, we include additional steps 14-17 to consider two scenarios in Algorithm H: **(1)** reweighting based on the connections of training neighbors to training neighbors and **(2)** reweighting based on the connections of training neighbors to validation neighbors. We experiment on Collab to compare the performance of these two scenarios in Table 12. We can see the performance of reweighting based on validation neighbors is higher than reweighting based on training neighbors. This demonstrates that the validation neighbors are more connected to the testing neighbors, justifying the existence of the topological distribution shift.

Table 12: Comparing the link prediction performance on Collab between reweighting based on training neighbors and reweighting based on validation neighbors

Performance	GCN			SAGE		
	No	Train	Val	No	Train	Val
Hits@5	18.94±1.20	19.48±0.75	**22.36±0.32**	11.25±1.24	20.52±2.35	**24.34±0.07**
Hits@10	31.24±3.44	32.69±1.00	**35.15±2.42**	26.41±1.88	31.23±3.52	**37.15±2.44**
Hits@50	50.12±0.22	52.77±1.00	**53.24±0.22**	49.68±0.25	51.87±0.10	**52.69±0.26**
Hits@100	54.44±0.49	56.89±0.17	**57.28±0.10**	54.69±0.18	56.59±0.19	**57.27±0.25**

L EXPLAINING WHY THE CURVE OF LINK PREDICTION PERFORMANCE HAS SEVERAL FAST DOWN IN FIGURE 7(A)

Here we delve deep into the reason why we encounter several fast-down performances in Figure 7(a). We ascribe it to the weight clip[3]. We hypothesize that the loss landscape has several local minimums and hence by weight clipping with higher upper bound constraints, our learning step would be also larger so that the model could jump out of its original local optimum and keep finding some other better local optimum, which corresponds to the fast downtrend (first jump away from one local minimum and then find another better local minimum). We further empirically verify our hypothesis by visualizing the performance curve for each training process with different clipping weights in Figure 23. We can clearly see that as the clipping threshold becomes lower (upper bound decreases), we observe less fast downtrend decreases.

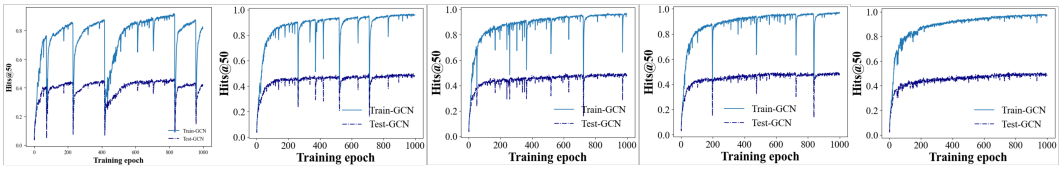

(a) No Clip (b) Clip 1.5 (c) Clip 1.0 (d) Clip 0.5 (d) Clip 0.2

Figure 23: From left to right, we constrain GCN-based link predictor with fewer upper bounds by clipping using a lower threshold. We can see the number of performance fast downtrend decreases. We hypothesize that the loss landscape has several local minimums and hence by weight clipping with lower upper bounds, our learning step would be also smaller so that the model could not jump out of its origin local optimum and hence we end up with fewer fast downtrends.

[3]Following the publically available implementation on GCN/SAGE on Collab link prediction, we employ the weight clip every time after parameter update